RESEARCH ARTICLE OPEN ACCESS

Band structure engineering of type I GaAs/AlAs nanostructure superlattice for near infrared detection

D. Barkissy, A. Nafidi, A. Boutramine, H. Charifi, A. Saba, H. Chaib
Laboratory of Condensed Matter Physics and Nanomaterials for Renewable Energy, Faculty of Sciences, University Ibn Zohr, Agadir, Morocco

ABSTRACT
We report here the electronic properties of GaAs/$Ga_{1-x}Al_xAs$, type I superlattices for x=1, performed in the envelope function formalism. We have studied the indirect-direct band gap transition in asymmetric $(GaAs)_{14}$ /$(AlAs)_m$ superlattices. Our calculations are confirmed by different experimental measurements. We have also studied the effect of the valence band offset, the temperature and the barrier thickness on the band structure of GaAs (d_1=3.95 nm)/AlAs (d_2=2.37 nm) superlattice. These results are in good agreement with reflectance measurements reported in literature. Finally, in the investigated temperature range, the cut-off wavelength is 716 nm $\leq \lambda_c \leq$ 755 nm situates this sample as near infrared detector.

Keywords **-** Envelope function formalism, GaAs/$Ga_{1-x}Al_xAs$ type I superlattices, III-V semiconductors, Band gap energy, Near infrared detector.

I. INTRODUCTION

Since the earlier works of Esaki and Tsu [1], the semiconductor superlattices (SLs) composed of alternating thin layers of two different semiconductors, have attracted considerable attention in both fundamental studies and many applications like detectors, medical diagnostics, thermography and other fields applications. This is due to the fact that, the properties of these artificial materials can be different from those of their individual alloys. The development of growth techniques such as molecular beam epitaxy (MBE), has made significant advances in the conception of various compound semiconductors nanostructures superlattices. Among them, III-V superlattices (GaAs/ $Ga_{1-x}Al_xAs$ [1-2] - type I), III-V superlattices (InAs/GaSb [3] - type II) and II-VI superlattices (HgTe/CdTe [4] - type III).

The realization of $(GaAs)_n/(AlAs)_m$ nanostructures superlattices, where n and m denote, respectively, the number of GaAs (well) and AlAs (barrier) monolayers in one period, was associated with several efforts to determine the electronic band structure and other properties of such materials. Therefore, different investigations have predicted and confirmed the existence of indirect-direct band gap transition for a certain range of thicknesses. For example, the calculations of Schulman and McGill [5], using the tight binding approach, show direct gap for symmetric (n=m) superlattices with $n \geq 2$. Nakayama and Kamimura [6] made calculations, with n=m ranged from 1 to 4, using a self consistent pseudo-potential method and predicts an indirect gap superlattice for the n=1 and a direct gap for the others ($n \geq 2$). Later, Yamaguchi [7] have used the tight binding method and reported that for n=m=1, 2, 3, 4, and 5 the superlattices have an indirect band gap, while for n=7 to 20 have direct gap. In addition, Fujimoto et al. [8] have used the tight binding method on a symmetric superlattices with n=m ranged from 1 to 15 at room temperature and shows the existence of indirect-direct band gap transition at n=8. On the other hand, the photoluminescence measurements of Ishibashi et al. [9], under atmospheric pressure at 300 K, 77 K and 4.2 K on a number of symmetric samples (n=m=1 to 24), predict a direct band gap for $n \geq 2$. But, Guohua Li et al. [10] have shown, by photoluminescence measurements under atmospheric pressure at both 300 K and 77 K, that this transition takes place at n=m=11. This shows the effect of the superlattice period on their electronic band structure. However, by comparing the results of these different theoretical calculations and experimental measurements, maybe we can notice a significant confusion.

In this paper, we report the results of type I; GaAs/$Ga_{1-x}Al_xAs$ superlattices electronic properties with x=1. The transition indirect-direct band gap in asymmetric ($n \neq m$) superlattices, as well as the effect of temperature and the barrier thickness on the band gap energy, performed by the envelope function formalism.

II. SUPERLATTICES BAND STRUCTURE THEORY

The calculations of band structure for type I superlattices, can be performed by the envelope function formalism [4, 11]. Here, we used the

valence band offset Λ, between heavy holes bands edges of GaAs and AlAs at the center of first Brillouin zone (Γ point), Λ=560 meV measured by Wolford et al. [12], using the photoluminescence measurements.

The general expression of the dispersion relation for light particles (electron and light hole) subbands of the superlattice is defined by [4]:

$$\cos[k_z(d_1+d_2)] = \cos(k_1 d_1)\cos(k_2 d_2) - \frac{1}{2}[(\xi+\frac{1}{\xi}) + \frac{k_p^2}{4k_1k_2}(r+\frac{1}{r}-2)]\sin(k_1 d_1)\sin(k_2 d_2) \quad (1)$$

Where the subscripts 1 and 2 refer to GaAs and AlAs, respectively. k_z is the wave vectors in the direction of growth axis and $k_p(k_x,k_y)$ is the wave vector in plane of the superlattice which describes the motion of particles perpendicular to k_z. In our case;

$$\xi = \frac{k_1}{k_2} r \text{ and } r = \frac{E-\varepsilon_2}{E-\varepsilon_1-\Lambda}$$

E is the energy of the light particles in the superlattice measured from the top of the Γ_8 valence band of AlAs bulk, while ε_i (i =1 or 2) is the interaction band gaps $E(\Gamma_6)$ - $E(\Gamma_8)$ in the bulk GaAs and AlAs, respectively (Fig.1).

At given energy, the two–band Kane model [13] gives the wave vector $(k_i^2+k_p^2)$ in each host material:

$$\begin{cases} \frac{2}{3}P_1^2\hbar^2(k_1^2+k_p^2) = (E-\varepsilon_1-\Lambda)(E-\Lambda) & \text{for GaAs} \\ \frac{2}{3}P_2^2\hbar^2(k_2^2+k_p^2) = E(E-\varepsilon_2) & \text{for AlAs} \end{cases}$$

The relationship between Kane matrix element P and Kane energy E_p is given by the expression [14]:

$$P^2 = \frac{E_p}{2m_0}$$

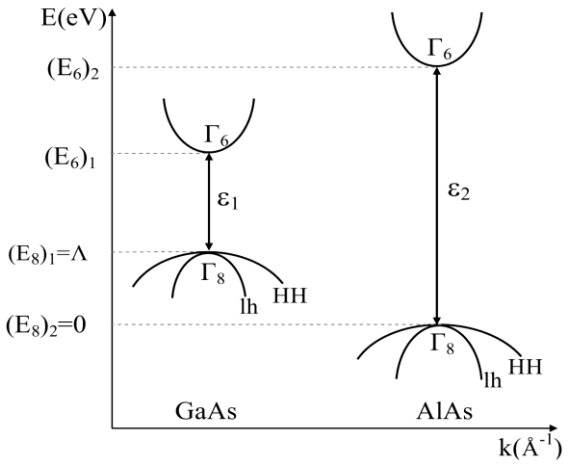

Fig.1: Illustration of different parameters related to the electronic band structure. $(E_6)_i$ and $(E_8)_i$ where i=1,2 are the conduction and the valence bands energies of GaAs and AlAs bulks, respectively.

Where E_{p1}=28.8 eV and E_{p2}=21.1 eV are the Kane energy of GaAs and AlAs, respectively.

For a given energy E, the superlattice state exists if the right-hand side of the dispersion relation lies in the range [-1, 1] that implies $-\pi/d \le k_z \le \pi/d$ in the first Brillouin zone, where $d=d_1+d_2$ is the superlattice period.

The superlattice heavy hole subbands are obtained from the same equation (1) with:

$$\xi = \frac{k_1}{k_2} r, \; r = \frac{m_{HH}^{*2}}{m_{HH}^{*1}} \text{ and}$$

$$\begin{cases} \frac{\hbar^2}{2m_{HH}^{*1}}(k_1^2+k_p^2) = (E-\Lambda) & \text{for GaAs} \\ \frac{\hbar^2}{2m_{HH}^{*2}}(k_2^2+k_p^2) = E & \text{for AlAs} \end{cases}$$

Where $m_{HH}{}^{*1}=0.34m_0$ is the GaAs heavy hole effective mass, evaluated by Molenkamp et al. [15] using high-resolution excitation spectra and K.P calculations on a set of multiple-quantum-well structures. For bulk AlAs, $m_{HH}{}^{*2}=0.75m_0$ were measured by the spherically averaged mass measurements [16].

In this work, we used the energy band gaps of AlAs bulk, measured by Monemar [17] with photoluminescence excitation spectra at T=300 K, respectively, at X and Γ points: $\varepsilon_2(X)$=2.153 eV and $\varepsilon_2(\Gamma)$=3.03 eV. For GaAs: $\varepsilon_1(X)$=1.978 eV [18] and $\varepsilon_1(\Gamma)$=1.422 eV as reported by Estrera et al. [19] using photoreflectance measurements at room temperature.

The electronic structures and energy gap computation consists of solving the previous dispersion relations with the reported parameters.

III. RESULTS AND DISCUSSION

The $(GaAs)_n/(AlAs)_m$ superlattices studied here consists of alternating n monolayers of GaAs and m monolayers of AlAs (with one monolayer thickness is nearly around 2.83 Å [18]). It is well known that for GaAs, the lowest energy level in the conduction band is located at Γ point (the center of the first Brillouin zone), while it is at X point for AlAs, which is lower than X-valley energy of GaAs, due to the interface band offsets. In this case, the lowest conduction band energy is located at X point (the edge of the Brillouin zone), these structures called indirect superlattices, defined by $E_g(X)$ indirect band gap energy.

We illustrate in the Fig.2, the calculated band gap energy at Γ point $E_g(\Gamma)$ and X point $E_g(X)$, as a function of AlAs thicknesses (in monolayers n), at room temperature for asymmetric $(GaAs)_{14}/(A1As)_m$ superlattices with fixed GaAs layer number n=14.

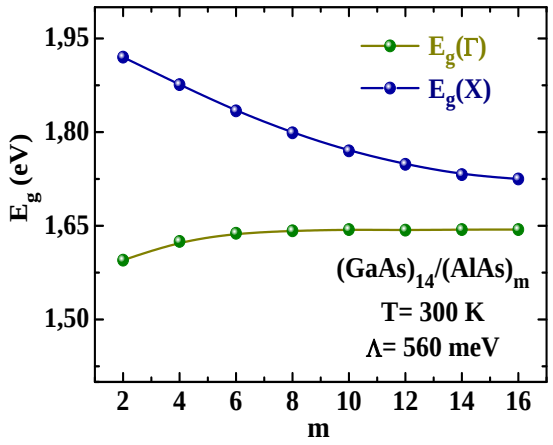

Fig.2: The calculated band gap energy of asymmetric $(GaAs)_{14}/(AlAs)_m$ superlattices.

As we can see for n=14 and $2 \leq m \leq 16$ the band gap $E_g(\Gamma)$, which is corresponding to the difference between the bottom of the conduction band and the top of the valence band at Γ-valley, is lower than $E_g(X)$. In this case, for any barrier thickness, the superlattice has direct band gap.

These results are in agreement with the photoluminescence experiments of Litovchenko et al. [19] on non symmetric GaAs/AlAs superlattices, for which the ratio of well to barrier thickness is at least 2, have shown to exhibit a direct band gap.

We will study a sample with $d_1(GaAs)=39.5$ Å and $d_2(AlAs)=23.7$ Å corresponding to $(GaAs)_{14}/(AlAs)_8$ direct band gap superlattice. Consequently, $d_1/d_2=1.66$ and $d=d_1+d_2=63.2$ Å is the period of the superlattice.

In the Fig.3 we illustrate the energy E of the conduction (E_i), first light-hole (h_1) and the heavy-hole (HH_i) subbands as a function of d_2 at room temperature for $d_1=1.66\ d_2$. The case of this sample ($d_2=23.7$ Å) is indicated by the vertical dashed line.

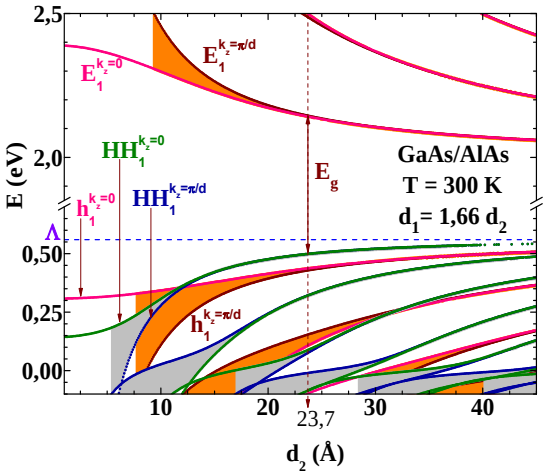

Fig.3: Energy position of the conduction and valence subbands at 300 K in both the center Γ ($k_z=0$) and the limit ($k_z= \pi/d$) of the first Brillouin zone as a function of AlAs barrier thickness d_2.

The calculated band gap energy, from the bottom of the first conduction subband (E_1) to the top of the first valence subband (HH_1) at T=300 K is $E_g(\Gamma)=E_1$ - $HH_1=1.643$ eV. This result is in good agreement with the reported one by Humlek et al. [20]; $E_g=1.647$ eV, using reflectance measurements at T=298 K, without indicating the value of the valence band offset. According to our calculation, we assume that Λ=560 meV of such sample.

As presented in Fig.4, the band gap energy $E_g(\Gamma)$ increases with the valence band offset Λ and presents a maximum near Λ=390 meV with $E_g=1.653$ eV for T=300 K, then it decreases when the valence band offset increases.

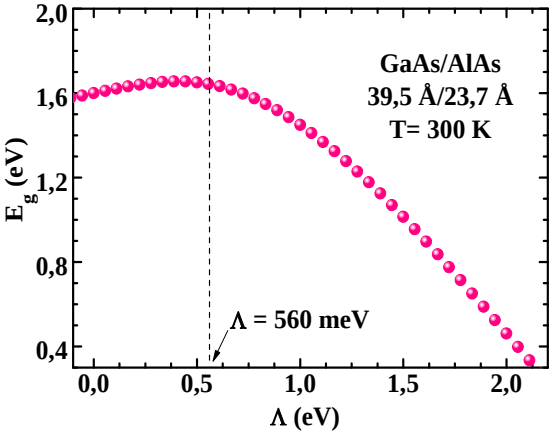

Fig.4: The band gap $E_g(\Gamma)$ at the center Γ, as function of valence band offset Λ.

We show in the Fig.5, the calculated band gap energy E_g (blue stars) of this superlattice, as a function of temperature, in a range of 4 K to 300 K. The calculated band gaps decreased from 1,732 eV to 1,643 eV for 4 K and 300 K, respectively. These results are in good agreement with the reflectance measurements (green solid circles) of Humlek et al. [20].

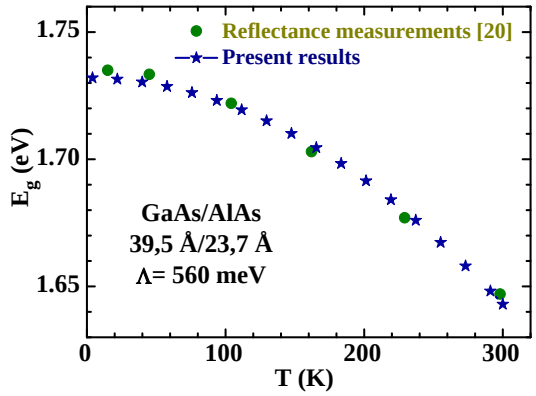

Fig.5: The temperature dependence of the band gap energy $E_g(\Gamma)$. In the figure, blue stars illustrate our calculated data and the solid green circles represent the

reflectance measurements of Humlek et al.[20] for comparison.

We can see that at low temperature E_g changes hardly and decreases as the temperature is increased. This behavior can be attributed to the increased thermal energy which let the amplitude of atomic vibrations increases. Then, the interatomic spacing increases and the potential seen by the electrons decreases, leading to a smaller band gap [21].

We should note here that the effect of temperature on the band gap energy of type I SLs is different from that of type III studied in previous work [22], where E_g of HgTe/CdTe SLs increases with temperature.

In addition our calculated results obey to the Varshni empirical expression, which associate the band gap energy of SL with temperature [23]:

$$E_g(T) = E_{0K} - \alpha \frac{T^2}{T+\beta}$$

Where $E_g(T)$ is the band gap energy at the temperature T, E_{0K} is the energy gap at absolute zero, α and β are empirical fitting parameters. So, by the fitting procedure of the superlattice band gap dependence on temperature (Fig.5), we find out the following values: E_{0K}=1.7328 eV, α=0,00058 eV/K and β=281 K.

As shown in Fig.6, the calculated band gap energy E_g as a function of barrier thickness d_2 at T=300 K tends to decrease with increasing barrier width. When d_2 increases from around 14 to 24 Å, our theoretical results shown by blue solid circles, decrease from 1.840 eV to 1.642 eV, in agreement with the Kronig-Penney model calculations made by Humlek et al. [20] at T=298 K. For shorter thicknesses (d_2 < 14 Å), we can see that, the findings results diverge and the difference becomes about 196 meV at 6 Å.

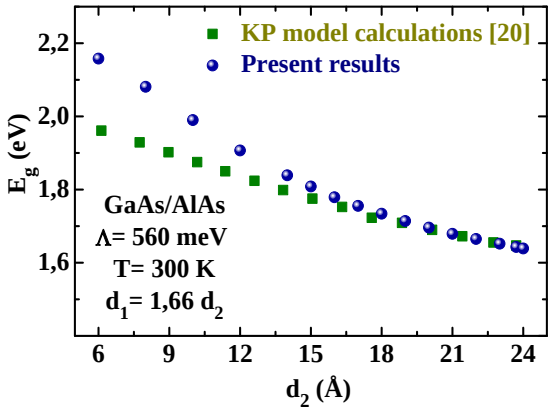

Fig.6: The calculated band gap versus the barrier thickness. In the figure our results (blue solid circles) and the calculated data with Kronig-Penney (KP) model (solid green squares), read from a graph of Ref.[20] for comparison.

However, it is well known that the Kronig-Penney models do not consider the interface effects; which consist of coupling between conduction and valence bands of different bulks due to the superlattice potential. The KP model can provide good results for type I superlattices composed of wide band gap semi-conductors, but not adequate for type II and type III SLs, such as InAs/GaSb [24] and HgTe/CdTe [21], in which there is an extensive bands mixing. On the other hand, the decreasing in the band gap energy with increasing barrier thickness can be explained by the fact that the number of atoms in the crystallite grows which affects the bands formed by the merger of nearest energy levels. Consequently, the number of overlapping orbitals between adjacent atoms increases. As result, the valence and conduction bands separation starts to narrow, resulting in a reduction of the band gap [25].

The calculated band gap energy E_g and the cut-off wavelength λ_c, as a function of d_2, are shown in Fig.7.

We calculated the detection cut-off wavelength λ_c using the expression:

$$\lambda_c(nm) = \frac{1240}{E_g(eV)}$$

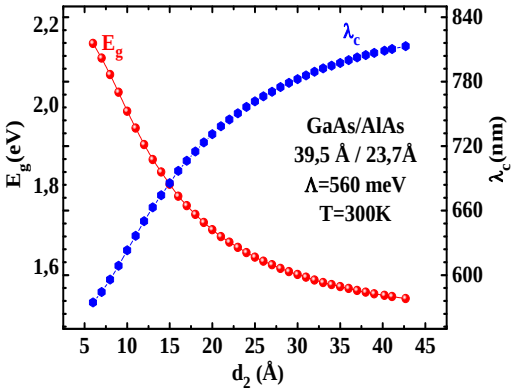

Fig.7: The band gap E_g and cut-off wavelength λ_c, at the center Γ, as a function of the barrier AlAs thickness at room temperature.

From Fig.7, we can see that, the band gap energy $E_g(\Gamma)$ decreases when AlAs thickness increases. Therefore, when d_2 increases from 6 Å to 42,7 Å the fundamental band gap energy decreases from 2,158 eV to 1.525 eV.

The corresponding cut-off wavelength increases with d_2, from 575 nm to 814 nm at 300 K, which is located in the near infrared region [26].

Finally, in the investigated temperature range of 4 K to 300 K, the cut-off wavelength of the concerned superlattice GaAs (d_1=39.5 Å)/AlAs (d_2=23.7 Å) is: 716 nm < λ_c < 755 nm situates this sample as near infrared detector.

IV. CONCLUSION

In this paper, we have reported the electronic properties of a two-dimensional GaAs/AlAs superlattice at room temperature. In our case, d_1=39.5 Å and d_2=23.7 Å. The envelope function formalism, used here, predicts that the value of fundamental band gap energy at 300 K is 1.643 eV. Beside this, we have studied the effect of the valence band offset, the barrier thickness and the temperature on the band gap energy of the SL. We found that E_g decreases with the previous factors. Those results are in agreement with the experimental measurements of Humlek et al. According to our calculations Λ= 560 meV.

We have also studied the indirect-direct transition in asymmetric $(GaAs)_{14}/(AlAs)_m$ SLs with m ranged from 2 to 16. We observed that $(GaAs)_{14}/(AlAs)_m$ are always a direct band gap SLs in the motioned range. Those results were confirmed by different experimental measurements.

Finally, for the investigated GaAs/AlAs superlattice in a range of 4 K to 300 K the corresponding cut-off wavelength is 716 nm < λ_c < 755 nm situates this sample as near infrared detector.

REFERENCES

[1] L. Esaki and R. Tsu, Superlattice and Negative Differential Conductivity in Semiconductors, *IBM Journal of Research and Development*, 14 (1), 1970, 61–65.

[2] R. Dingle, A.C. Gossard, and W. Wiegmann, Direct Observation of Superlattice Formation in a Semiconductor Heterostructure, *Physical Review Letters*, 34, 1975, 1327–1330.

[3] G. A. Sai-Halasz, R. Tsu, and L. Esak, "A new semiconductor superlattice," *Applied Physics Letters*, 30, 1977, 651.

[4] G. Bastard, Theoretical investigations of superlattice band structure in the envelope-function approximation, *Physical Review B*, 25, 1982, 7584–7597.

[5] J. N. Schulman and T. C. McGill, Band Structure of AlAs-GaAs (100) Superlattices, *Physical Review Letters*, 39, 1977, 1680.

[6] T. Nakayama and H. Kamimura, Band Structure of Semiconductor Superlattices with Ultrathin Layers $(GaAs)_n/(AlAs)_n$ with n=1, 2, 3, 4, *Journal of the Physical Society of Japan*. 54, 1985, 4726-4734.

[7] E. Yamaguchi, Theory of the DX Centers in III-V Semiconductors and (001) Superlattices, *Journal of the Physical Society of Japan*, 56, 1987, 2835-2852.

[8] H. Fujimoto, C. Hamaguchi, T. Nakazawa, K. Taniguchi, K. Imanishi, H. Kato, and Y. Watanabe, Direct and indirect transition in $(GaAs)_n/(AlAs)_n$ superlattices with n=1-15, *Physical Review B*, 41, 1990, 7593.

[9] A. Ishibashi, Y. Mori, M. Itabashi and N. Watanabe, "Optical properties of $(AlAs)_n/(GaAs)_n$ superlattices grown by metalorganic chemical vapor deposition," *Journal of Applied Physics*. 58, 1985, 2691.

[10] Guohua Li, D. Jianga, H. Hana, Z. Wanga and K. Ploog, Investigation of the electronic structures of $(GaAs)_n/(AlAs)_n$ short period superlattices by photoluminescence spectroscopy under hydrostatic pressure, *Journal of Luminescence*, 46, 1990, 261-270.

[11] G. Bastard, Superlattice band structure in the envelope-function approximation, *Physical Review B*, 24, 1981, 5693-5697.

[12] D. J. Wolford, *Proceedings of the 18th International Conference on the Physics of Semiconductors*, Stockholm, Sweden, 1986, 1115.

[13] Evan O. Kane, Band structure of indium antimonide, *Journal of Physics and Chemistry of Solids*, 1(4), 1957, 249-261.

[14] G.Bastard, *Wave mechanics applied to semiconductor heterostructures* (Les Editions de Physique, Paris, 1988).

[15] L. W. Molenkamp, R. Eppenga, G. W. 't Hooft, P. Dawson, C. T. Foxon, and K. J. Moore, Determination of valence-band effective-mass anisotropy in GaAs quantum wells by optical spectroscopy, *Physical Review B*, 38, 1988, 4314.

[16] O. Madelung, U. Rössler and M. Schulz, Al(x)Ga(1-x)As, effective masses, deformation potentials and related parameters Properties, *Landolt Börnstein Group III Condensed Matter*, (Berlin: Springer-Heidelberg, 2002), 1-11.

[17] B. Monemar, Fundamental Energy Gaps of AlAs and Alp from Photoluminescence Excitation Spectra, *Physical Review B*, 8, 1973, 5711.

[18] S. Adachi, *GaAs and Related Materials, Bulk Semiconducting and Superlattice Properties*, (World Scientific, Singapore, 1994).

[19] V. G. Litovchenko, D. V. Korbutyak, A. I. Bercha, Yu. V. Kryuchenko, S. G. Krylyuk, H. T. Grahn, R. Hey and K. H. Ploog, Observation of stimulated emission in an ultrashort-period nonsymmetric GaAs/AlAs superlattice, *Applied Physics Letters*, 78, 2001, 4085.

[20] J. Humlek, F. Luke, and K. Ploog, Temperature dependence of the direct energy gap in a GaAs/AlAs superlattice, *Physical Review B*, 42, 1990, 2932.

[21] Hilmi Ünlü, A thermodynamic model for determining pressure and temperature effects

on the bandgap energies and other properties of some semiconductors, *Solid State Elecronics*, 35(9), 1992, 1343-1352.

[22] M. Braigue, A. Nafidi, A. Idbaha, H. Chaib, H. Sahsah, M. Daoud, B. Marí Soucase, M. Mollar García, K. Chander Singh and B. Hartiti, Correlation Between Band Structure and Magneto-Transport Properties in HgTe/CdTe Two-Dimensional Far-Infrared Detector Superlattice, *Journal of Low Temperature Physics*, 171, 2013, 808-817.

[23] Y. P. Varshni, Temperature dependence of the energy gap in semiconductors, *Physica*, 34, 1967, 149.

[24] A. Boutramine, A. Nafidi, D. Barkissy, A. Eddiouane and H.Chaib, Electronic bands structure and gap in mid-infrared detector InAs/GaSb type II nanostructure superlattice, to be published (2015).

[25] S. V. Gaponenko, *Optical Properties of Semiconductor Nanocrystals*, (Cambridge University Press, Cambridge, 1998).

[26] Nibir K. Dhar, Ravi Dat and Ashok K. Sood, Advances in Infrared Detector Array Technology, in Prof. Sergei Pyshkin (Ed.), *Optoelectronics - Advanced Materials and Devices*, 7 (Croatia: InTech, 2013) 149-188.